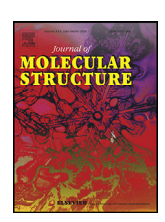
ELSEVIER

Contents lists available at ScienceDirect

Journal of Molecular Structure

journal homepage: www.elsevier.com/locate/molstr



Synthesis, kinetic evaluation and molecular docking studies of donepezil-based acetylcholinesterase inhibitors



Makar Makarian^a, Michael Gonzalez^a, Stephanie M. Salvador^a, Shahrokh Lorzadeh^b, Paula K. Hudson^a, Stevan Pecic^{a,*}

- ^a Department of Chemistry and Biochemistry, California State University, Fullerton, USA
- ^b Department of Human Anatomy and Cell Science, Rady Faculty of Health Sciences, Max Rady College of Medicine, University of Manitoba, Winnipeg, MB R3E 019. Canada

ARTICLE INFO

Article history: Received 2 May 2021 Revised 3 August 2021 Accepted 31 August 2021 Available online 3 September 2021

Keywords:
Alzheimer's disease
Donepezil
Microwave-assisted synthesis
Structure-activity relationship
Enzyme inhibition
Acetylcholinesterase
Molecular modeling

ABSTRACT

In an effort to develop new therapeutic agents to treat Alzheimer's disease, a series of donepezil-based analogs were designed, synthesized using an environmentally friendly route, and biologically evaluated for their inhibitory activity against electric eel acetylcholinesterase (AChE) enzyme. *In vitro* studies revealed that the phenyl moiety of donepezil can be successfully replaced with a pyridine ring leading to equally potent inhibitors of electric eel AChE. Further kinetic evaluations of the most potent inhibitor showed a dual-binding (mixed inhibition) mode, similar to donepezil. Molecular modeling studies suggest that several additional residues could be involved in the binding of this inhibitor in the human AChE enzyme active site compared to donepezil.

© 2021 The Author(s). Published by Elsevier B.V. This is an open access article under the CC BY-NC-ND license (http://creativecommons.org/licenses/by-nc-nd/4.0/)

1. Introduction

Alzheimer's disease (AD) is a neurodegenerative disease characterized by memory loss, dementia and cognitive impairment in elderly populations [1–5]. Acetylcholinesterase (AChE) is an important enzyme that hydrolyses the neurotransmitter acetylcholine at cholinergic synapses in both the central nervous system and peripheral nervous system [6]. It has been observed that the progression of AD is complex and connected with multiple hallmarks such as the destruction of cholinergic nerves in the brain and decreased levels of acetylcholine (ACh), accumulation of amyloid β $(A\beta)$ plaques, oxidative stress, dyshomeostasis of metal ions, mitochondrial malfunction and many others [7-11]. According to the cholinergic hypothesis, AChE inhibitors represent a promising therapeutic strategy for treating the symptoms of AD [12,13]. To date, there are three AChE inhibitors approved by the Food and Drug Agency where donepezil (Fig. 1) is the most commonly used [14]. However, the approved AChE inhibitors are associated with several adverse effects and are used for the treatment of only mild to moderate symptoms in the early stages of AD [15,16].

* Corresponding author.

E-mail address: specic@fullerton.edu (S. Pecic).

Current approaches in the treatment of AD are focused in developing Designed Multiple Ligands (DMLs) [17], small molecules specifically designed to simultaneously interact with several biological targets involved in the pathogenesis of AD [18]. Given the complex and multifactorial etiology of AD, this approach, also known as polypharmacology, can be highly beneficial for future AD therapeutic strategies. Many of these multitargeted efforts utilize acetylcholinesterase as one of the targets [19–21]. Therefore, there is clearly an interest for the development of new AChE inhibitors with improved potencies that can be used in future multitarget drug discoveries of novel AD therapeutics.

The active site of the AChE enzyme is composed of the peripheral binding site, a deep and narrow gorge called the peripheral anionic site (PAS), and the catalytic site, which is formed by three amino acids: serine (S203), histidine (H447) and glutamic acid (E334) [22,23]. It is believed that PAS serves as a recognition site for the substrate acetylcholine, and the important amino acid involved in binding the substrate is tryptophan (W286) [24]. Another important residue involved in intermolecular interactions with the substrate ACh is tryptophan (W86) and is located in the proximity of the catalytic triad S203-H447-E334 [25]. Donepezil, the selective AChE inhibitor clinically used to treat AD, interacts with both PAS and catalytic site [26].

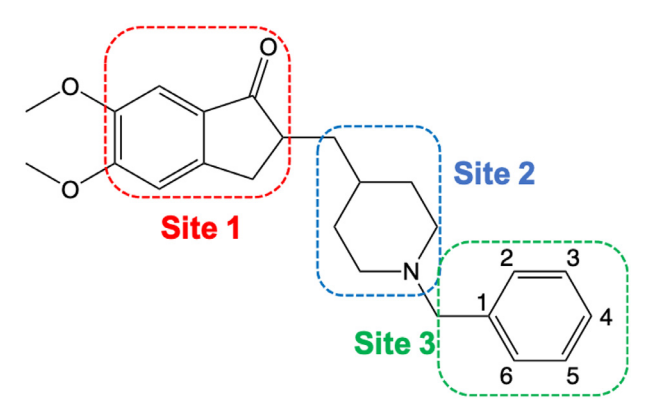


Fig. 1. The structure of Donepezil and SAR study sites.

Here we describe the design, synthesis, and structure-activity relationship (SAR) study of new AChE inhibitors based on the donepezil structure using electric eel AChE enzyme, a convenient and well-studied model [24,25]. We also report the kinetic studies, molecular docking experiments and several predicted pharmacokinetic properties for the most potent compound discovered in this study.

2. Results and discussion

2.1. Design and synthesis

Previously, several structure-activity relationship (SAR) studies have been reported for the clinically approved acetylcholinesterase inhibitor donepezil [27–29]. Together with X-ray crystallographic data (PDB ID: 4EY7), it was found that an indanone moiety (Site 1 - shown in red, Fig. 1) is responsible for binding to the peripheral

anionic site (PAS) of AChE via aromatic π - π stacking interactions [26], while the piperidine ring (Site 2 - shown in blue, Fig. 1) interacts with the amino acid tyrosine (Y337) located in the anionic part of catalytic active site (Fig. 2) [30,31]. The benzyl moiety (Site 3 - shown in green, Fig. 1) of donepezil is in close proximity of tryptophan (W86), and two amino acids, H447 and S203, both part of the catalytic triad [32]. Previously it has been shown that modification of the benzene ring of Site 3 can lead to a strong AChE inhibition [27]. Thus, we decided to design new AChE inhibitors with modifications at Site 3. Although, there were numerous and extensive SAR studies of donepezil in the past 25 years [27,33], interestingly, only a few studies explore the effects on AChE inhibition with replacement of the benzyl group with a pyridylmethyl group [34,35]. In order to further investigate how the addition of a nitrogen to Site 3 will affect the inhibition potencies, we started with the design of analogs 1-3 (Table 1). We hypothesized that the introduction of the basic nitrogen to the molecule, which will be protonated at a physiological pH, will provide an additional ionic- π interaction within the catalytic site of AChE and lead to more potent inhibitors. Next, we explored the effects on the inhibition potency of the more bulky quinolyl moiety with the design of analog 4. In addition, we designed eight analogs with modifications of the pyridyl ring with fluoro-, chloro-, bromo-, and methyl- substituents placed at various positions, as represented with analogs 5-12.

The synthetic route for synthesis of the donepezil analogs 1–12 is shown in Scheme 1. The reductive amination of commercially available 5,6-dimethoxy-2-(4-piperidinylmethyl)-1-indanone and corresponding aldehydes, using sodium triacetoxyborohydride as a reductive agent and microwave irradiation for 20 min at 80 °C, furnished the target analogs 1–12 in moderate yields. The structures and purity of the final compounds were characterized by proton and carbon NMR spectroscopy (See Supplemental information) and high-resolution mass spectrometry (HRMS).

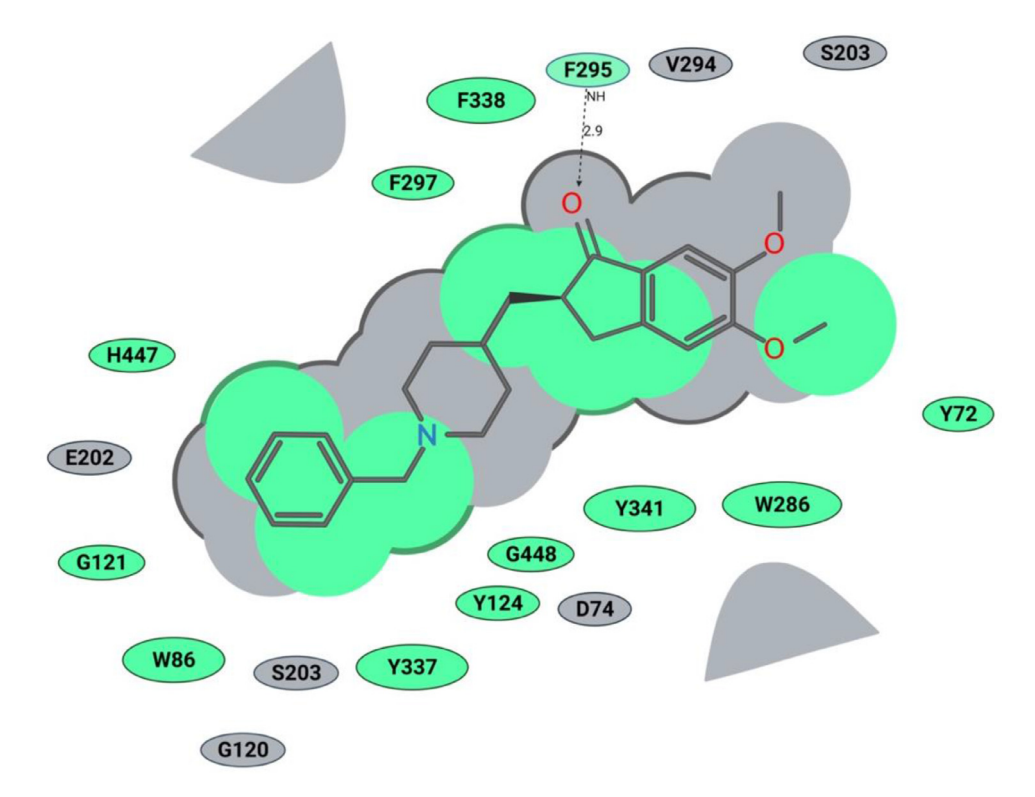


Fig. 2. Binding of Donepezil in the human AChE active site (2D representation): green shading represents hydrophobic regions; gray parabolas represent accessible surfaces for large areas; gray dotted lines represent hydrogen bonds; the broken thick line around the **donepezil** shape indicates accessible surface; the size of residue ellipses represents the strength of the contact.

Scheme 1. Reagents and conditions: NaBH(CH₃COO)₃, DCM, MW irradiation, 20 min, 80 °C.

2.2. Biological evaluation

All synthesized analogs, and donepezil as the control inhibitor, were tested for inhibitory activity on electric eel AChE enzyme using Ellman's spectrophotometric method [36]. The inhibition potencies of analogs 1-12 for AChE enzyme are summarized in Table 1. Our SAR study started with the evaluation of the analogs **1–3**. We noticed that the introduction of the basic nitrogen into position 2 and 4 of phenyl ring (Fig. 1) led to 20- and 8-fold decreases in potency relative to donepezil. Analog 2, on the other hand, with the nitrogen atom in position 3, led to inhibitory potency comparable to donepezil, with an IC₅₀ value of 51 nM. This SAR exploration suggests that enhanced potency of analog 2, compared to analogs 1 and 3, is not due to increased polarity and basicity from the nitrogen atom, but rather due to the location of the nitrogen atom, and thus being better tolerated within the active site at position 3 of the phenyl ring. It also shows the importance of aromatic hydrogens in positions 2 and 4, but further investigations at these positions are needed to assess the particular role of these substituents with the inhibition potencies. Next, we introduced a quinoline ring as shown in analog 4, which led to the moderate inhibition potency of AChE, with an IC50 value of 356 nM. Although the quinoline moiety led to decreased inhibition potency compared to donepezil, the quinoline ring offers access to many diverse chemical substituents that could improve AChE inhibition which will be explored in the future SAR studies. Placement of chloro- and bromo- substituents in position 3 of the 4-pyridyl ring, as shown in analogs 5 and 6, led to low micromolar inhibitory potency relative to donepezil. On the other hand, placement of a chloro- group in position 2 of the 4-pyridyl moiety (analog 7), was better tolerated and led to a moderate inhibition potency, with an IC₅₀ value of 364 nM. The introduction of the 2,6-disubstitution for chloro- group (analog 8) led to significant decrease in the inhibitory potency on the AChE enzyme. Adding fluoro-, chloro-, and bromo- groups in position 2 of the 3-pyridyl moiety, as shown in analogs 9-11, did not improve activity and led to higher IC50 values relative to donepezil. This suggests that the steric effects of these groups probably coupled with electronic effects play an important role in the binding to the enzyme and contribute negatively to the inhibition potency for this set of analogs. Similarly, placement of a methyl- group in position 4 of the 3-pyridyl ring (analog 12), was not well tolerated and led to the high nanomolar inhibition potency, with an IC₅₀ value of 928 nm.

However, encouraged with the inhibition potency of analog **2**, we decided to further explore the mechanism of inhibition of this analog. The kinetic studies of the electric eel AChE enzyme for the substrate acetylthiocholine in the presence of analog **2** were performed using Ellman's method as described in the Experimental section. Analysis of a Lineweaver-Burke double reciprocal plot of 1/velocity versus 1/substrate (Fig. 3) shows that slopes are increasing at increasing concentrations of analog **2**, and are intersecting above the *x*-axis, indicating mixed-type inhibition, i.e., binding to both PAS and the catalytic active site of AChE. Dual-binding site

character is also reported for donepezil [26]. Using a Dixon plot, a linear transformation of reciprocal enzyme rates vs. inhibitor concentrations (Fig. 4), we were able to calculate a K_i value of 62 nM for analog **2**. Since the human AChE and electric eel AChE sequences share 60% sequence identity (Fig. S1), and are significantly similar in the region of the catalytic active site, we expect that analog **2** will have similar binding modes in PAS and the catalytic site of human AChE, and probably similar strong inhibition potency in the nanomolar range.

2.3. In silico studies

To further understand and predict binding modes of donepezil analogs 1-12 with human AChE we conducted molecular docking studies. Using the ICM Pro Molsoft software package, we first prepared the enzyme structure using standard ICM Pro guidelines, and subsequently performed molecular docking of donepezil analogs 1-12 and donepezil. The obtained docking scores (Table 1) and visual inspection of their binding modes suggested that all analogs synthesized in this study should not have any steric or not-allowed contacts with the binding site of human AChE. Next, we compared the binding modes of donepezil and analog 2 within the active site of human AChE. We observed the benzyl ring of donepezil (Fig. 2) in the proximity of tryptophan (W86), with possible π - π stacking. We also noticed possible interactions with amino acids S203 and H447, both part of the AChE catalytic triad. Next, we observed a hydrogen bonding of donepezil's carbonyl group with phenylalanine (F295), acting as a hydrogen bond donor. The middle part of donepezil, the piperidine ring, interacts with Y337 and D74, while the indanone ring is located near to W286, F295, F338 and Y341, making strong hydrophobic interactions. Based on our molecular docking experiment, the binding of analog 2 is very similar to donepezil, but more complex (Fig. 5). The pyridylmethyl group is also located in the proximity of tryptophan (W86), and the two amino acids that are part of the catalytic triad, S203 and H447. We also observed that pyridylmethyl moiety interacts with G121, E202 and G448. In addition, we noticed a spacious open pocket where the nitrogen of pyridine ring is located, suggesting that this analog will probably be well accommodated in the human AChE active site (Figs. 5 and 6). The piperidine ring and indanone moiety both have very similar interactions as donepezil, and we also noticed the same hydrogen bonding with phenylalanine (F295). Finally, analog 2 showed a similar docking score as donepezil, thus, further in vitro evaluation of this promising analog in human AChE enzyme should be performed in the future.

Using the ICM Pro Chemistry software, we calculated several important ADMET properties of the most potent inhibitor identified in this study, analog **2**, in comparison to donepezil. Since our therapeutic target is located in the brain, we first decided to determine whether the potential drug candidate will penetrate the blood brain barrier (BBB). A BBB prediction score above 4 indicates that the tested compound can pass the BBB [37]. Both, analog **2** and donepezil had BBB scores greater then **4**, 4.93 and 5.28, re-

Table 1AChE inhibitory activities of Analogs 1–12.

Compound	R	IC ₅₀ s (nM)	Docking Score	
	~~~~			
Analog 1	N	793	-18.4	
Analog 2	N	51	-17.63	
Analog 3		334	-17.24	
Analog 4		356	-12.67	
Analog 5	N	2064	-16.24	
Analog 6	N Br	1796	-16.22	
Analog 7	CI	364	-13.42	
Analog 8	CI	4318	-14.01	
Analog 9	F	718	-14.28	
Analog 10	CI	414	-13.59	
Analog 11	Br	1116	-16.11	

(continued on next page)

Table 1 (continued)

Compound	R	IC ₅₀ s (nM)	Docking Score	
Analog 12	N	928	-13.07	
Donepezil		44	-17.57	

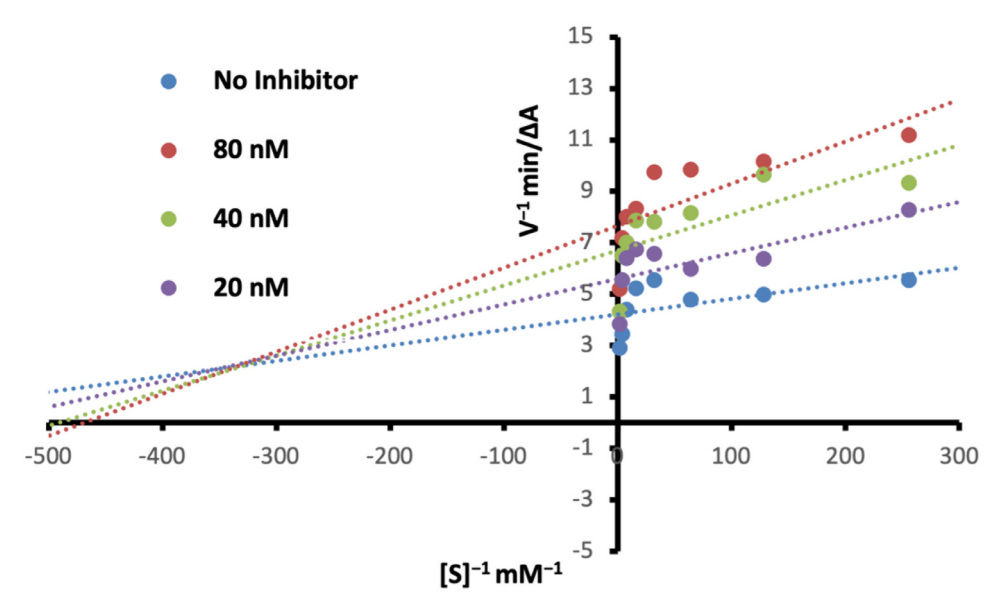


Fig. 3. Lineweaver-Burke double reciprocal plot for Analog 2.

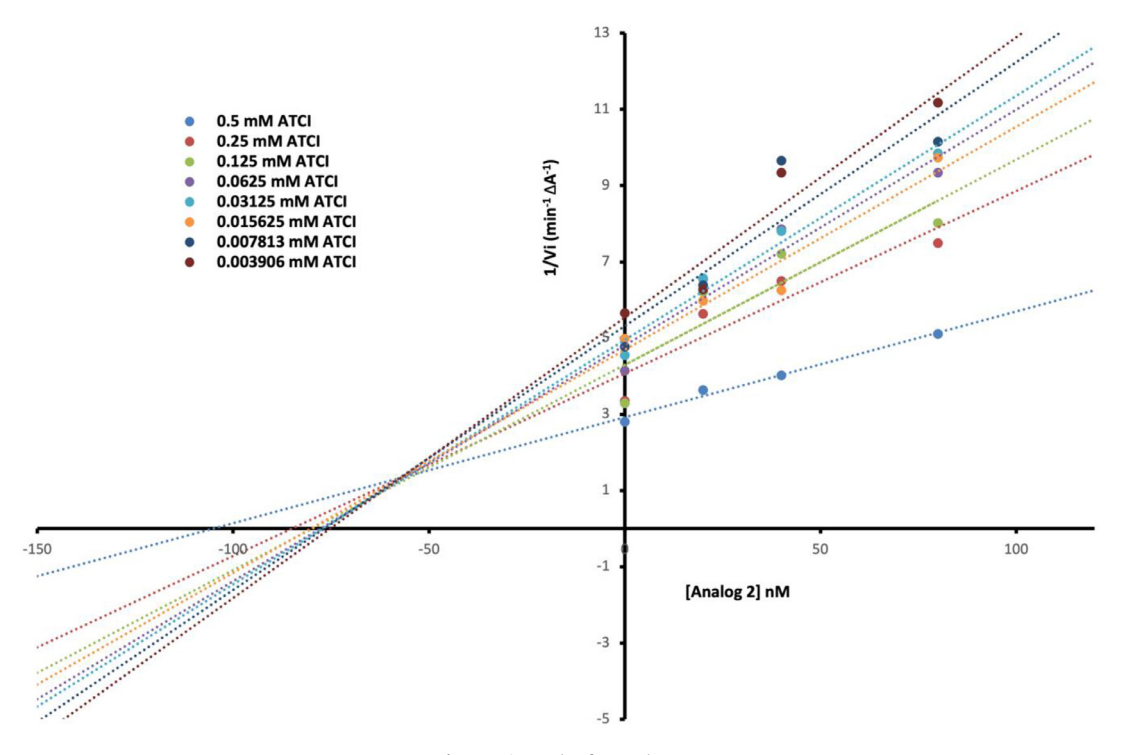
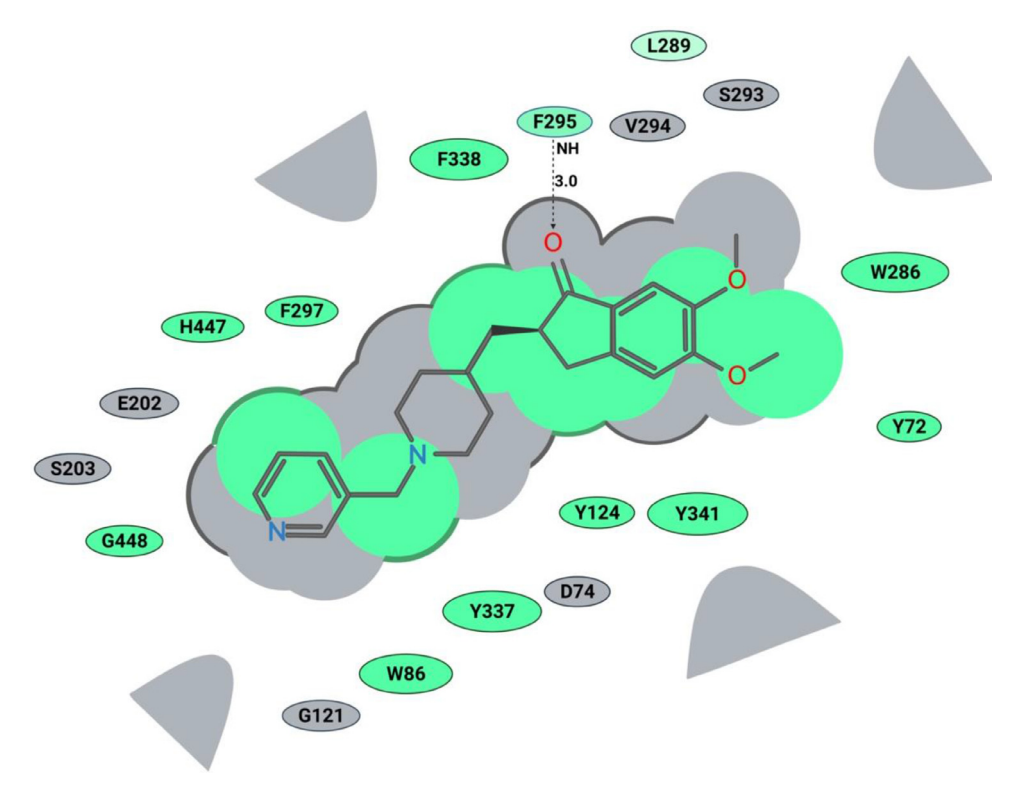


Fig. 4. Dixon plot for Analog 2.



**Fig. 5.** Binding of Analog 2 in human AChE active site (2D representation): green shading represents hydrophobic region; gray parabolas represent accessible surfaces for large areas; gray dotted lines represent hydrogen bond; the broken thick line around analog **2** shape indicates accessible surface; the size of residue ellipses represents the strength of the contact. (For interpretation of the references to color in this figure legend, the reader is referred to the web version of this article).

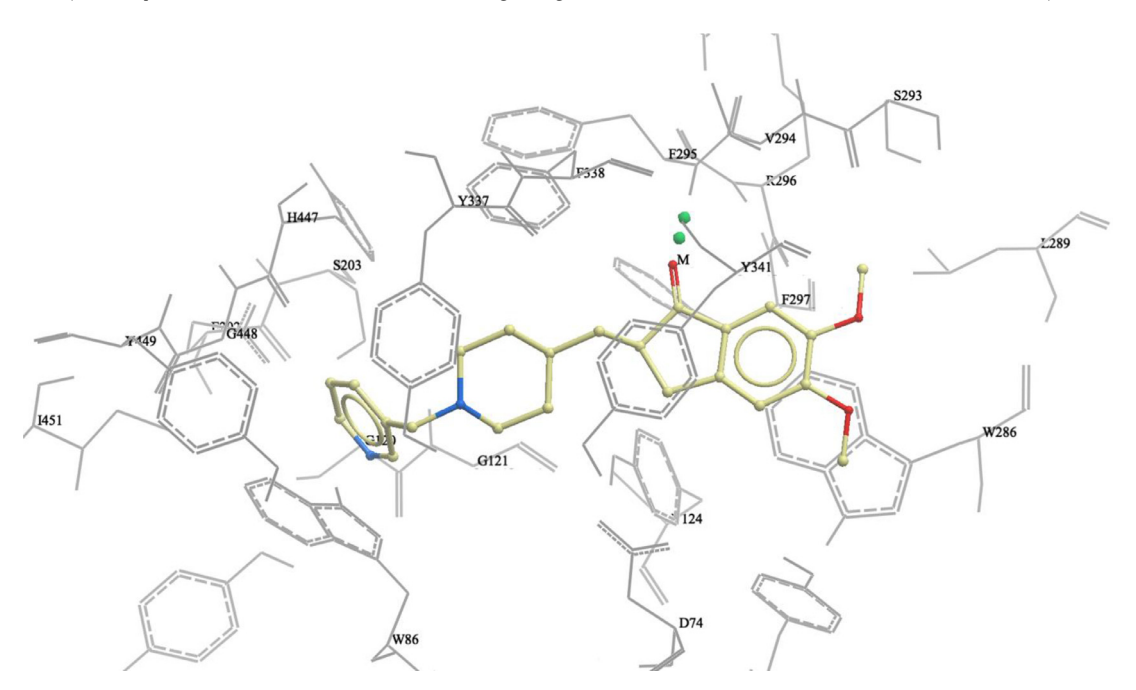


Fig. 6. Binding of Analog 2 in human AChE active site (3D representation).

spectively, suggesting that both drugs will cross the BBB (Table 2). Next, we wanted to estimate if analog **2** will have a relative likelihood to be administrated orally. According to *Lipinski's rule of five* [38], an orally active drug has no more than one violation of the following criteria: (1) molecular weight under 500 daltons (Da); (2) no more than 5 hydrogen bond donors; (3) no more than 10 hydrogen bonds acceptors; and (4) an octanol-water partition coefficient log P of less than 5. According to our calculations, analog

**2** would be considered as a potential oral drug as it doesn't violate any of the four abovementioned rules: the molecular weight is 380.488 Da, it has no hydrogen bond donors, has six hydrogen bond acceptors and the calculated log P is 3.17. Using *Veber et al.'s rule* [39], we investigated the drug absorption of analog **2**. Molecular flexibility and polar surface play an important role in drug absorption, namely, too many rotatable bonds (above 10) and a polar surface area (PSA) above 140 Angstroms, are not good pa-

**Table 2**Predicted ADMET properties for Analog 2 and Donepezil.

Compound	BBB Score	No. of HBA	No. of HBD	Molecular Weight	cLogP	PSA	No. of Rotatable Bonds	HALF-LIFE (hours)	hERG	Tox Score	Tox Groups	LD ₅₀ (mg/kg)
Analog 2	4.93	6	0	380.488	3.17	41.91	6	6.72	0.54	0	N/A	412
Donepezil	5.28	5	0	379.500	4.46	32.39	6	6.72	0.45	0	N/A	344

rameters for drug absorption according to Veber's rule. Analog 2 has 6 rotatable bonds and a PSA of 41.91 Å suggesting good absorption. Since orally absorbed drugs pass through the liver before they are distributed to the rest of the body, we were interested in calculating the half-life of the analog 2. Our predictions show that analog 2 would probably undergo a similar metabolic pathway as donepezil, since we found the same half-life value of 6.72 h for both compounds. Finally, we analyzed the potential toxicity, by calculating the hERG binding prediction, Tox scores and  $LD_{50}$ . Oral toxicity prediction results show that analog 2 has  $LD_{50}$ value of 412 mg/kg, comparing to donepezil with predicted LD₅₀ value of 344 mg/kg. According to the ICM Pro guidelines, hERG values above 0.5 suggest that the tested compound will likely exhibit some hERG inhibition at 100  $\mu$ M or less. Our calculations show that analog 2 has a hERG value slightly above the reference value, 0.54, while donepezil is slightly below 0.5. Nevertheless, since it has inhibition potency in the nanomolar range, we believe that analog 2 represents a good candidate as a follow up lead compound. In addition, Tox score of 0, suggest that there are no potentially toxic groups or reactive chemical functionalities present in analog 2.

## 3. Conclusion

Herein, we present the discovery of a new AChE inhibitor analog **2**, having an IC₅₀ in the range of the FDA-approved drug donepezil. Our kinetic studies determined that this inhibitor binds to the enzyme as a mixed-type inhibitor, binding to both the peripheral anionic site (PAS) and catalytic active site, similar to donepezil. Molecular docking experiments not only revealed the potential binding position and interactions of this analog in the binding pocket of human AChE but also that the pyridylmethyl moiety could successfully replace the benzyl ring of donepezil without steric or other interferences. Analog **2** also satisfies several predicted pharmacokinetic and pharmacodynamic parameters suggesting that this inhibitor should be further tested in the human AChE enzyme and used as guide for future SAR studies.

## 4. Material and methods

All solvents and reagents were obtained from Sigma–Aldrich, Matrix Scientific, TCI, and Acrōs Organic and used without further purification. Analytical thin-layer chromatography (TLC) was performed on aluminum plates precoated with silica gel, also obtained from Sigma–Aldrich. Column chromatography was carried out on Merck 938S silica gel, and a Teledyne CombiFlash Rf Flash Chromatography system. Proton and carbon NMR spectra were recorded with a Bruker 400 MHz NMR spectrometer. Spectra were referenced to the residual solvent peak: proton chemical shifts are reported relative to the residual solvent peak (chloroform = 7.26 ppm) as follows: chemical shift ( $\delta$ ), proton ID, multiplicity (s = singlet, bs = broad singlet, d = doublet, bd = broad doublet, dd = doublet of doublets, t = triplet, q = quartet, m = multiplet, integration, coupling constant(s) in Hz). Carbon chemical shifts are reported relative to the resid-

ual deuterated solvent signals (chloroform = 77.2 ppm). Melting points were measured with a MEL-TEMP II melting point apparatus and are reported uncorrected. All compounds described were > 95% purity. Purity was confirmed by high-resolution liquid chromatography mass spectrometer (ThermoFisher Ultimate 3000 binary UPLC coupled to a Q Exactive Focus Orbitrap mass spectrometer). The elution gradient increased from acetonitrile:water (20:80 + 0.1% formic acid) to acetonitrile:water (70:30 + 0.1% formic acid) over 3 min and held for one minute at a flow rate of 0.4 mL/min. Microwave reactions were carried out in a CEM Discover SP microwave synthesizer. Electric eel AChE enzyme (Type VI-S, lyophilized powder, Item No. C3389) was obtained from Sigma Aldrich. Molecular modeling studies and docking experiments were performed using ICM Pro Molsoft software.

## 4.1. Experimental

## 4.1.1. Chemistry

General procedure for the preparation of donepezil analogs: 5,6-Dimethoxy-2-(4-piperidinylmethyl)-1-indanone, HCl salt (680 mg) was dissolved in a 25 mL aqueous solution of saturated sodium bicarbonate (NaHCO₃) and a 25 mL of ethyl acetate. It was stirred vigorously for approximately 25 min and the organic layer was separated. The aqueous layer was washed twice with 25 mL dichloromethane, the organic layers were combined, dried over anhydrous sodium sulfate and concentrated. Freebased 5,6dimethoxy-2-(4-piperidinylmethyl)-1-indanone was obtained as a pale orange solid (350 mg). 0.86 mmol of the freshly freebased 5,6dimethoxy-2-(4-piperidinylmethyl)-1-indanone, sodium triacetoxyborohydride (2.58 mmol), and corresponding aldehyde (0.86 mmol) were dissolved in 20 mL of anhydrous dichloromethane. The reaction mixture was subjected to microwave irradiation at 80 °C for 20 min. The mixture was transferred to a separatory funnel and the organic layer was washed with an aqueous solution of saturated NaHCO₃ (20 mL). The organic layer was then dried over anhydrous sodium sulfate, filtered and concentrated. The crude product was purified by column chromatography (using 2-5% methanol/dichloromethane or 1:1 ethyl acetate/hexane solvent systems) or using a CombiFlash chromatography system.

**5,6-dimethoxy-2-((1-(pyridin-2-ylmethyl)piperidin-4-yl)methyl)-2,3-dihydro-1***H***-inden-1-one, Analog 1**: 2-pyridinecarboxaldehyde was used as a starting material to obtain **1** as a clear thick oil (40% yield);  1 H NMR (400 MHz, CDCl $_3$ )  $\delta$  8.53 (s, 1H), 7.63 (t, J = 7.2 Hz, 1H), 7.43 (d, J = 6.8 Hz, 1H), 7.14 (s, 2H), 6.83 (s, 1H), 3.93 (s, 3H), 3.88 (s, 3H), 3.66 (s, 2H), 3.25–3.19 (m, 1H), 2.93 (s, 2H), 2.68 (d, J = 14 Hz, 2H), 2.12–2.08 (m, 2H), 1.75–1.65 (m, 1H), 1.54–1.29 (m, 4H).  13 C NMR (100 MHz, CDCl $_3$ ):  $\delta$  207.6, 155.4, 149.4, 149.1, 148.7, 136.3, 129.3, 123.3, 122.0, 107.3, 104.4, 64.8, 56.2, 56.1, 54.0, 45.4, 38.6, 34.2, 33.3, 32.8, 31.6 ppm. HRMS-ESI+: calculated for  $C_{23}H_{28}N_2O_3$  + H: 381.2178; Found: 381.2169.

**5,6-dimethoxy-2-((1-(pyridin-3-ylmethyl)piperidin-4-yl)methyl)-2,3-dihydro-1***H***-inden-1-one, Analog 2**: 3-pyridinecarboxaldehyde was used as a starting material to obtain **2** as a pale yellow oil (73% yield);  1 H NMR (400 MHz, CDCl₃)  $\delta$  8.53–8.51 (m, 2H), 7.72 (d, J = 7.6 Hz, 1H), 7.29–7.27 (m, 1H),

7.17 (*s*, 1H), 6.86 (*s*, 1H), 3.96 (*s*, 3H), 3.91 (*s*, 3H), 3.56 (*s*, 2H), 3.27–3.21 (*m*, 1H), 2.94–2.50 (*m*, 1H), 2.70 (*m*, 2H), 2.07–2.02 (*m*, 3H), 1.94–1.90 (*m*, 1H), 1.73 (*t*, *J* = 16.4 Hz, 2H), 1.53 (*d*, *J* = 8 Hz, 1H), 1.43–1.30 (*m*, 3H).  13 C NMR (100 MHz, CDCl₃):  $\delta$  207.7, 155.5, 150.4, 149.5, 148.7, 148.5, 137.1, 133.4, 129.3, 123.4, 107.3, 104.4, 60.3, 56.2, 56.1, 53.6, 45.3, 38.6, 34.2, 33.4, 32.6, 31.5 ppm. HRMS-ESI+: calculated for C₂₃H₂₈N₂O₃ + H: 381.2178; Found: 381.2166.

**5,6-dimethoxy-2-((1-(pyridin-4-ylmethyl)piperidin-4-yl)methyl)-2,3-dihydro-1***H***-inden-1-one, Analog 3**: 4-pyridinecarboxaldehyde was used as a starting material to obtain **3** as a yellowish oil (69% yield);  1 H NMR (400 MHz, CDCl₃)  $\delta$  8.52 (d, J = 6 Hz, 2H), 7.27 (t, J = 6.8 Hz, 2H), 7.16 (s, 1H), 6.85 (s, 1H), 3.95 (s, 3H), 3.89 (s, 3H), 3.48 (s, 2H), 3.23 (dd, J = 9.2, 8 Hz, 1H), 2.87–2.82 (m, 2H), 2.72–2.67 (m, 2H), 2.04–1.98 (m, 2H), 1.93–1.89 (m, 1H), 1.75–1.66 (m, 2H), 1.53–1.49 (m, 1H), 1.38–1.30 (m, 3H).  13 C NMR (100 MHz, CDCl₃):  $\delta$  207.7, 155.5, 149.6, 149.4, 148.7, 148.0, 129.2, 123.9, 121.1, 107.3, 104.4, 62.0, 56.2, 56.1, 53.9, 45.4, 38.6, 34.2, 33.3, 32.9, 31.7 ppm. HRMS-ESI+: calculated for C₂₃H₂₈N₂O₃ + H: 381.2178; Found: 381.2167.

5,6-dimethoxy-2-((1-(quinolin-4-ylmethyl)piperidin-4-yl)methyl)-2,3-dihydro-1*H*-inden-1-one, Analog 4quinolinecarboxaldehyde was used as a starting material to obtain **4** as a clear oil (38% yield); ¹H NMR (400 MHz, CDCl₃)  $\delta$ 8.87 (d, I = 4.4 Hz, 1H), 8.26 (d, I = 7.6 Hz, 1H), 8.13 (d, I = 8Hz, 1H), 7.72 (t, I = 6.8 Hz, 1H), 7.57 (t, I = 6.8 Hz, 1H), 7.46 (d, J = 4.4 Hz, 1H, 7.18 (s, 1H), 6.87 (s, 1H), 3.97 (s, 3H), 3.93 (s, 2H),3.92 (s, 3H), 3.25 (dd, J = 9.2, 8 Hz, 1H), 2.96 (t, J = 10.4 Hz, 2H), 2.75-2.69 (m, 2H), 2.13 (t, J = 11.2 Hz, 2H), 1.97-1.91 (m, 1H), 1.79–1.69 (*m*, 2H), 1.61–1.51 (*m*, 1H), 1.45–1.32 (*m*, 3H). ¹³C NMR (100 MHz, CDCl₃):  $\delta$  207.7, 155.5, 150.1, 149.5, 148.7, 148.3, 144.6, 129.9, 129.3, 129.0, 127.7, 126.2, 124.1, 121.1, 107.3, 104.4, 59.8, 56.2, 56.1, 54.3, 45.4, 38.7, 34.3, 33.3, 33.1, 31.9 ppm. HRMS-ESI+: calculated for  $C_{27}H_{30}N_2O_3 + H$ : 431.2335; Found: 431.2325.

**2-((1-((2-chloropyridin-4-yl)methyl)piperidin-4-yl)methyl)**-**5,6-dimethoxy-2,3-dihydro-1***H***-inden-1-one, Analog 5**: 2-chloroisonicotinaldehyde was used as a starting material to obtain **5** as a thick colorless oil (27% yield); ¹H NMR (400 MHz, CDCl₃)  $\delta$  8.30 (*s*, 1H), 7.32 (*s*, 1H), 7.20 (*s*, 1H), 7.16 (*s*, 1H), 6.85 (*s*, 1H), 3.95 (*s*, 3H), 3.90 (*s*, 3H), 3.47 (*s*, 2H), 3.27–3.21 (*m*, 1H), 2.83 (*s*, 2H), 2.70 (*d*, *J* = 14 Hz, 2H), 2.02 (*t*, *J* = 11.2 Hz, 2H), 1.91 (*t*, *J* = 10.8 Hz, 1H), 1.76–1.67 (*m*, 2H), 1.51 (bs, 1H), 1.41–1.25 (*m*, 3H). ¹³C NMR (100 MHz, CDCl₃):  $\delta$  207.6, 155.5, 151.9, 151.7, 149.4, 148.7, 129.3, 124.0, 122.5, 107.3, 104.4, 61.5, 65.2, 56.1, 53.9, 45.4, 38.6, 34.1, 33.3, 32.9, 31.8. HRMS-ESI+: calculated for C₂₃H₂₇ClN₂O₃ + H: 415.1788; Found: 415.1778.

**2-((1-((2-bromopyridin-4-yl)methyl)piperidin-4-yl)methyl)**- **5,6-dimethoxy-2,3-dihydro-1***H*-**inden-1-one, Analog 6**: 2-bromo-4-pyridinecarboxaldehyde was used as a starting material to obtain **6** as a tan oil (53% yield);  1 H NMR (400 MHz, CDCl₃)  $\delta$  8.26 (s, 1H), 7.46 (s, 1H), 7.22 (s, 1H), 7.14 (s, 1H), 6.84 (s, 1H), 3.94 (s, 3H), 3.88 (s, 3H), 3.44 (s, 2H), 3.22 (dd, J = 9.6, 8 Hz, 1H), 2.81 (s, 2H), 2.68 (d, J = 14 Hz, 2H), 2.00 (t, J = 11.2 Hz, 2H), 1.90 (s, 1H), 1.75–1.66 (m, 2H), 1.50 (t bs, 1H), 1.39–1.23 (t m, 3H). t C NMR (100 MHz, CDCl₃): t 207.6, 155.5, 151.7, 149.9, 149.4, 148.7, 142.4, 129.2, 127.2, 127.8, 122.9, 107.4, 104.4, 61.4, 56.2, 56.1, 53.9, 45.3, 38.6, 34.1, 33.3, 32.9, 31.8. HRMS-ESI+: calculated for t C₂₃H₂₇BrN₂O₃ + H: 459.1283; Found: 459.1274.

**2-((1-((3-chloropyridin-4-yl)methyl)piperidin-4-yl)methyl) 5,6-dimethoxy-2,3-dihydro-1***H***-inden-1-one, Analog 7: 3-chloroisonicotinaldehyde was used as a staring material and 7 was obtained as a white solid (30% yield); mp = 122-125 °C; ^1H NMR (400 MHz, CDCl₃) \delta 8.50 (s, 1H), 8.43 (d, J= 4.8 Hz, 1H), 7.48 (d, J = 5 Hz, 1H), 7.16 (s, 1H), 6.86 (s, 1H), 6.85 (s, 1H), 3.95 (s, 3H), 3.90 (s, 3H), 3.58 (s, 2H), 3.24 (q, J= 8.4 Hz, 1H), 2.89–2.84 (m, 2H), 2.70 (d, J= 14.4 Hz, 2H), 2.11 (t, J= 11.2 Hz, 2H), 1.96–** 

1.89 (m, 1H), 1.78–1.67 (m, 2H), 1.51 (bs, 1H), 1.43–1.31 (m, 3H).  13 C NMR (100 MHz, CDCl $_3$ ):  $\delta$  207.8, 155.7, 149.7, 149.3, 148.9, 147.9, 146.0, 131.9, 129.5, 124.5, 107.5, 104.6, 58.7, 56.4, 56.3, 54.3, 45.6, 38.9, 34.4, 33.5, 33.3, 32.1 ppm. HRMS-ESI+: calculated for  $C_{23}H_{27}ClN_2O_3$  + H: 415.1788; Found: 415.1780.

**2-((1-((3,5-dichloropyridin-4-yl)methyl)piperidin-4-yl)methyl)-5,6-dimethoxy-2,3-dihydro-1***H***-inden-1-one, Analog 8**: 3,5-dichloroisonicotinaldehyde was used as a starting material and **8** was obtained as a white solid (18% yield); mp = 162-164 °C;  1 H NMR (400 MHz, CDCl₃)  $\delta$  8.45 (s, 2H), 7.48 (d, J = 5 Hz, 1H), 7.16 (s, 1H), 6.84 (s, 1H), 3.95 (s, 3H), 3.89 (s, 3H), 3.69 (s, 2H), 3.22 (q, J = 8.4 Hz, 1H), 2.89–2.85 (m, 2H), 2.71–2.66 (m, 2H), 2.26–2.19 (m, 2H), 1.91–1.85 (m, 1H), 1.72–1.62 (m, 3H), 1.52 (bs, 1H), 1.33–1.20 (m, 4H).  13 C NMR (100 MHz, CDCl₃):  $\delta$  207.8, 155.6, 149.5, 148.8, 147.8, 143.3, 134.1, 129.4, 107.4, 104.5, 100.1, 56.3, 56.2, 56.1, 54.1, 45.5, 38.7, 34.4, 33.4, 33.1, 31.9 ppm. HRMS-ESI+: calculated for  $C_{23}H_{26}Cl_2N_2O_3$  + H: 449.1399; Found: 449.1389.

**2-((1-((2-fluoropyridin-3-yl)methyl)piperidin-4-yl)methyl)- 5,6-dimethoxy-2,3-dihydro-1***H***-inden-1-one, Analog <b>9**: 2-fluoronicotinaldehyde was used as a starting material and **9** was obtained as a clear oil (56% yield);  1H  NMR (400 MHz, CDCl₃)  $\delta$  8.11 (d, J = 4.8 Hz, 1H), 7.87 (t, J= 9.2 Hz, 1H), 7.20-7.17 (m, 2H), 6.86 (s, 1H), 3.97 (s, 3H), 3.91 (s, 3H), 3.56 (s, 2H), 3.24 (q, J= 8.4 Hz, 1H), 2.91–2.87 (m, 2H), 2.73–2.69 (m, 2H), 2.12–2.05 (m, 2H), 1.95–1.88 (m, 1H), 1.78–1.67 (m, 2H), 1.49 (bs, 1H), 1.38–1.30 (m, 3H).  13 C NMR (100 MHz, CDCl₃):  $\delta$  207.6, 155.4, 149.4, 148.7, 145.9, 145.8, 141.4, 129.2, 121.3, 120.6, 107.4, 104.5, 56.2, 56.0, 55.1, 53.6, 45.4, 38.6, 34.2, 33.2, 33.0, 31.8 ppm. HRMS-ESI+: calculated for  $C_{23}H_{27}FN_2O_3$  + H: 399.2084; Found: 399.2077.

**2-((1-((2-chloropyridin-3-yl)methyl)piperidin-4-yl)methyl) 5,6-dimethoxy-2,3-dihydro-1***H***-inden-1-one, Analog 10: 2-chloronicotinaldehyde was used as a starting material and 10 was obtained as a clear oil (44% yield); ^1H NMR (400 MHz, CDCl₃) \delta 8.27 (s, 2H), 7.91 (s, 2H), 7.25–7.24 (m, 1H), 7.16 (s, 1H), 6.86 (s, 1H), 3.96 (s, 3H), 3.90 (s, 3H), 3.61 (s, 2H), 3.24 (q, J= 8.4 Hz, 1H), 2.91-2.89 (m, 2H), 2.71 (d, J= 14.4 Hz 2H), 2.16 (t, J= 10.8 Hz 2H), 1.91 (bs, 1H), 1.79–1.68 (m, 2H), 1.59–1.24 (m, 5H). ^{13}C NMR (100 MHz, CDCl₃): \delta 207.6, 155.4, 150.9, 149.4, 148.6, 147.7, 129.2, 122.5, 107.3, 104.3, 58.7, 56.2, 56.0, 53.9, 45.3, 38.6, 34.1, 33.2, 32.9, 31.7, 29.6 ppm. HRMS-ESI+: calculated for C_{23}H_{27}ClN₂O₃ + H: 415.1788; Found: 415.1781.** 

**2-((1-((2-bromopyridin-3-yl)methyl)piperidin-4-yl)methyl) 5,6-dimethoxy-2,3-dihydro-1***H***-inden-1-one**, **Analog 11**: 2-bromonicotinaldehyde was used as a starting material and **11** was obtained as a clear oil (51% yield);  1 H NMR (400 MHz, CDCl₃)  $\delta$  8.26 (d, J= 4.8 Hz, 1H), 7.84 (d, J= 7.6 Hz, 1H), 7.28–7.25 (m, 2H), 7.18 (s, 1H), 6.87 (s, 1H), 3.97 (s, 3H), 3.92 (s, 3H), 3.57 (s, 2H), 3.26 (q, J= 8.2 Hz, 1H), 2.89 (t, J= 10.4 Hz, 1H), 2.74–2.71 (m, 2H), 2.19–2.13 (m, 2H), 1.97–1.91 (m, 1H), 1.80–1.68 (m, 3H), 1.55 (bs, 1H), 1.40–1.32 (m, 3H).  13 C NMR (100 MHz, CDCl₃):  $\delta$  207.7, 155.4, 149.4, 148.7, 148.1, 143.7, 138.5, 135.7, 129.3, 122.8, 107.3, 104.4, 60.9, 56.1, 54.0, 45.4, 38.6, 34.2, 33.2, 31.8 ppm. HRMS-ESI+: calculated for  $C_{23}H_{27}BrN_2O_3$  + H: 459.1283; Found: 459.1275.

**5,6-dimethoxy-2-((1-((6-methylpyridin-3-yl)methyl)piperidin-4-yl)methyl)-2,3-dihydro-1***H***-inden-1-one, Analog 12**: 6-methylnicotinaldehyde was used as a starting material and **12** was obtained as a clear oil (41% yield);  1 H NMR (400 MHz, CDCl₃)  $\delta$  8.36 (s, 1H), 7.56 (d, J = 6 Hz, 1H), 7.13–7.08 (m, 2H), 6.83 (s, 1H), 3.93 (s, 3H), 3.87 (s, 3H), 3.46 (s, 2H), 3.21 (q, J= 8.4 Hz, 1H), 2.88–2.84 (m, 2H), 2.68–2.65 (m, 2H), 2.51 (s, 3H), 2.00–1.95 (m, 2H), 1.90–1.84 (m, 1H), 1.73–1.64 (m, 2H), 1.49 (bs, 1H), 1.35–1.28 (m, 3H).  13 C NMR (100 MHz, CDCl₃):  $\delta$  207.6, 157.1, 155.4, 149.7, 149.4, 148.6, 137.2, 129.2, 122.8, 107.3, 104.3, 60.1, 56.1, 56.0, 53.6, 53.5, 45.3, 38.6, 34.2, 33.3, 32.7, 31.6, 24.0 ppm. HRMS-ESI+: calculated for  $C_{24}H_{30}N_2O_3$  + H: 395.2335; Found: 395.2329.

#### 4.1.2. AChE inhibition assays

AChE inhibition was determined using the Ellman et al.'s method [36] with acetylthiocholine iodide (ATCI) as a substrate. In brief, in a 96-well microplate, 45  $\mu$ L of electric eel AChE in assay buffer (400 U/L in 20 mM Tris-HCl, 150 mM NaCl, pH 7.5) was added to each of the wells, followed by 5  $\mu$ L of inhibitor dissolved in DMSO, and incubated at 24 °C for 15 min. Then, 150  $\mu$ L of the reaction mix (100 mM ATCI in water, 10 mM DTNB in ethanol and assay buffer) was added to each well and the absorbance was measured at 412 nm (A412). The absorbance was measured again at 412 nm after 10 min. Percent inhibition was calculated by comparing the rates for the samples relative to the blank (5  $\mu$ L DMSO instead of test compound solution) using the following formula: (1 –  $\Delta A$  Test Cpd / $\Delta A$  Blank) x 100%, where:  $\Delta A$  Test Cpd is the A412 value of a test compound well at 0 min subtracted from the A412 value of the same well at 10 min;  $\Delta A$  Blank is the A412 value of the DMSO Control well at 0 min subtracted from the A412 value of the DMSO Control well at 10 min. IC50 values were calculated by nonlinear regression analysis using GraphPad Prism software. Each experiment was performed in triplicate. Kinetic analysis of AChE inhibition was performed using the spectrophotometric method according to Ellman's procedure with some modifications [40]. In short, Lineweaver-Burke and Dixon plots were constructed at eight different concentrations of the substrate ATCI. Analog 2 was added to the assay buffer (20 mM Tris-HCl, 150 mM NaCl, pH 7.5) and pre-incubated with the electric eel AChE enzyme at 24 °C for 15 min, followed by the addition of ATCI. The assay solution containing analog 2 (1/2 IC₅₀, IC₅₀, 2xIC₅₀), DTNB (1 mM), AChE (400 Units/L) and ATCI (0.5, 0.25, 0.125, 0.0625, 0.03125, 0.015625, 0.0078125 and 0.00390625 mM) were dissolved in the assay buffer. Kinetic characterization of the hydrolysis of acetylthiocholine catalyzed by AChE was done at 412 nm. A parallel control experiment was carried out without the analog 2 in the mixture. Each experiment was performed in triplicate. Determination of the type of inhibition was assessed from Lineweaver-Burke. The  $K_i$  calculation was derived from the Dixon plot [41]. Data analysis was performed with GraphPad Prism software.

#### 4.1.3. Molecular modeling

For the docking studies of the donepezil analogs 1–12, a crystal structure of human acetylcholinesterase (AChE) enzyme complexed with donepezil (PDB ID: 4EY7) was used. PDB file 4EY7 was first converted to an ICM file and the inhibitor donepezil was removed. Docking experiments were performed following the program guidelines. ICM scores were obtained after this procedure. ADMET properties for all synthesized target analogs were calculated using the ICM Pro software.

## **Declaration of Competing Interest**

The authors declare that there is no conflict of interest regarding the publication of this article.

#### Acknowledgments

This research was financially supported by startup funds granted by the College of Natural Sciences and Mathematics at California State University, Fullerton, and 2020-2021 Junior/Senior Intramural Award, and, in part, by a grant from the National Institute of General Medical Sciences of the National Institutes of Health under Award Number SC2GM135020. The content is solely the responsibility of the authors and does not necessarily represent the official views of the National Institutes of Health. Instrumentation support was provided by the National Science Foundation MRI (CHE1726903) for acquisition of an UPLC-MS. We also thank Dr.

Terri Patchen (Student Creative Activities and Research) and Office of Research and Sponsored Projects at CSUF for their support.

#### Supplementary materials

Supplementary material associated with this article can be found, in the online version, at doi:10.1016/j.molstruc.2021.131425.

#### References

- [1] K. Sharma, Cholinesterase inhibitors as Alzheimer's therapeutics (Review), Mol. Med. Rep. 20 (2) (2019) 1479–1487.
- [2] J.M. Long, D.M. Holtzman, Alzheimer disease: an update on pathobiology and treatment strategies, Cell 179 (2) (2019) 312–339.
- [3] A. Behçet, T. Çağılılar, D. Barut Celepci, A. Aktaş, P. Taslimi, Y. Gök, M. Aygün, R. Kaya, İ. Gülçin, Synthesis, characterization and crystal structure of 2-(4-hydroxyphenyl)ethyl and 2-(4-nitrophenyl)ethyl substituted benzimidazole bromide salts: their inhibitory properties against carbonic anhydrase and acetylcholinesterase, J. Mol. Struct. 1170 (2018) 160–169.
- [4] P. Taslimi, İ. Gulçin, Antioxidant and anticholinergic properties of olivetol, J. Food Biochem. 42 (3) (2018) e12516.
- [5] F. Erdemir, D. Barut Celepci, A. Aktaş, P. Taslimi, Y. Gök, H. Karabıyık, İ. Gülçin, 2-Hydroxyethyl substituted NHC precursors: synthesis, characterization, crystal structure and carbonic anhydrase, α-glycosidase, butyrylcholinesterase, and acetylcholinesterase inhibitory properties, J. Mol. Struct. 1155 (2018) 797–806.
- [6] M.B. Colovic, D.Z. Krstic, T.D. Lazarevic-Pasti, A.M. Bondzic, V.M. Vasic, Acetyl-cholinesterase inhibitors: pharmacology and toxicology, Curr. Neuropharmacol. 11 (3) (2013) 315–335.
- [7] A. Serrano-Pozo, M.P. Frosch, E. Masliah, B.T. Hyman, Neuropathological alterations in Alzheimer disease, Cold Spring Harb. Perspect. Med. 1 (1) (2011) a006189-a006189.
- [8] M.A. Ansari, S.W. Scheff, Oxidative stress in the progression of Alzheimer disease in the frontal cortex, J. Neuropathol. Exp. Neurol. 69 (2) (2010) 155–167.
- [9] E.D. Roberson, L. Mucke, 100 years and counting: prospects for defeating Alzheimer's disease, Science 314 (5800) (2006) 781–784.
- [10] M.G. Savelieff, S. Lee, Y. Liu, M.H. Lim, Untangling amyloid-beta, tau, and metals in Alzheimer's disease, ACS Chem. Biol. 8 (5) (2013) 856–865.
- [11] S. Maramai, M. Benchekroun, M.T. Gabr, S. Yahiaoui, Multitarget therapeutic strategies for Alzheimer's disease: review on emerging target combinations, Biomed. Res. Int. 2020 (2020) 5120230.
- [12] R.T. Bartus, R.L. Dean, B. Beer, A.S. Lippa, The cholinergic hypothesis of geriatric memory dysfunction, Science 217 (4558) (1982) 408.
- [13] H. Hampel, M.M. Mesulam, A.C. Cuello, A.S. Khachaturian, A. Vergallo, M.R. Farlow, P.J. Snyder, E. Giacobini, Z.S. Khachaturian, Revisiting the cholinergic hypothesis in Alzheimer's disease: emerging evidence from translational and clinical research, J. Prev. Alzheimers Dis. 6 (1) (2019) 2–15.
- [14] Marucci, G.; Moruzzi, M.; Amenta, F., Chapter 31 Donepezil in the treatment of Alzheimer's disease. In Diagnosis and Management in Dementia, Martin, C. R.; Preedy, V. R., Eds. Academic Press: 2020; pp 495-510.
- [15] G. Marucci, M. Buccioni, D.D. Ben, C. Lambertucci, R. Volpini, F. Amenta, Efficacy of acetylcholinesterase inhibitors in Alzheimer's disease, Neuropharmacology (2020) 108352.
- [16] T.B. Ali, T.R. Schleret, B.M. Reilly, W.Y. Chen, R. Abagyan, Adverse effects of cholinesterase inhibitors in dementia, according to the pharmacovigilance databases of the United-States and Canada, PLoS ONE 10 (12) (2015) e0144337.
- [17] R. Morphy, Z. Rankovic, Designed multiple ligands. An emerging drug discovery paradigm, J. Med. Chem. 48 (21) (2005) 6523–6543.
- [18] L. Wang, G. Esteban, M. Ojima, O.M. Bautista-Aguilera, T. Inokuchi, I. Moraleda, I. Iriepa, A. Samadi, M.B. Youdim, A. Romero, E. Soriano, R. Herrero, A.P. Fernandez Fernandez, M. Ricardo Martinez, J. Marco-Contelles, M. Unzeta, Donepezil + propargylamine + 8-hydroxyquinoline hybrids as new multifunctional metal-chelators, ChE and MAO inhibitors for the potential treatment of Alzheimer's disease, Eur. J. Med. Chem. 80 (2014) 543–561.
- [19] K.S. Dias, C. Viegas, Multi-target directed drugs: a modern approach for design of new drugs for the treatment of Alzheimer's disease, Curr. Neuropharmacol. 12 (3) (2014) 239–255.
- [20] Z. Liu, L. Fang, H. Zhang, S. Gou, L. Chen, Design, synthesis and biological evaluation of multifunctional tacrine-curcumin hybrids as new cholinesterase inhibitors with metal ions-chelating and neuroprotective property, Bioorg. Med. Chem. 25 (8) (2017) 2387–2398.
- [21] K.S. Dias, C.T. de Paula, T. Dos Santos, I.N. Souza, M.S. Boni, M.J. Guimaraes, Silva, M. F., N.G. Castro, G.A. Neves, C.C. Veloso, M.M. Coelho, I.S. de Melo, F.C. Giusti, A. Giusti-Paiva, Silva, L. M., L.E. Dardenne, I.A. Guedes, L. Pruccoli, F. Morroni, A. Tarozzi, C. Viegas, Design, synthesis and evaluation of novel feruloyl-donepezil hybrids as potential multitarget drugs for the treatment of Alzheimer's disease, Eur. J. Med. Chem. 130 (2017) 440–457.
- [22] H. Dvir, I. Silman, M. Harel, T.L. Rosenberry, J.L. Sussman, Acetylcholinesterase: from 3D structure to function, Chem. Biol. Interact. 187 (1) (2010) 10–22.
- [23] Y. Zhang, J. Kua, J.A. McCammon, Role of the catalytic triad and oxyanion hole in acetylcholinesterase catalysis: an ab initio QM/MM study, J. Am. Chem. Soc. 124 (35) (2002) 10572–10577.
- [24] J.L. Sussman, M. Harel, F. Frolow, C. Oefner, A. Goldman, L. Toker, I. Silman, Atomic structure of acetylcholinesterase from Torpedo Californica: a prototypic acetylcholine-binding protein, Science 253 (5022) (1991) 872–879.

- [25] B.K. Taylor, D. Holloway, M.P. Printz, A unique central cholinergic deficit in the spontaneously hypertensive rat: physostigmine reveals a bradycardia associated with sensory stimulation, J. Pharmacol. Exp. Ther. 268 (3) (1994) 1081–1090.
- [26] J. Cheung, M.J. Rudolph, F. Burshteyn, M.S. Cassidy, E.N. Gary, J. Love, M.C. Franklin, J.J. Height, Structures of human acetylcholinesterase in complex with pharmacologically important ligands, J. Med. Chem. 55 (22) (2012) 10282–10286.
- [27] H. Sugimoto, Y. Iimura, Y. Yamanishi, K. Yamatsu, Synthesis and structure-activity relationships of acetylcholinesterase inhibitors: 1-benzyl-4-[(5,6-dimethoxy-1-oxoindan-2-yl)methyl]piperidine hydrochloride and related compounds, J. Med. Chem. 38 (24) (1995) 4821–4829.
- [28] P. Costanzo, L. Cariati, D. Desiderio, R. Sgammato, A. Lamberti, R. Arcone, R. Salerno, M. Nardi, M. Masullo, M. Oliverio, Design, synthesis, and evaluation of donepezil-like compounds as ACHE and BACE-1 inhibitors, ACS Med. Chem. Lett. 7 (5) (2016) 470–475.
- [29] R. Azzouz, L. Peauger, V. Gembus, M.L. Tintas, J. Sopkova-de Oliveira Santos, C. Papamicael, V. Levacher, Novel donepezil-like N-benzylpyridinium salt derivatives as AChE inhibitors and their corresponding dihydropyridine "bio-oxidizable" prodrugs: synthesis, biological evaluation and structure-activity relationship, Eur. J. Med. Chem. 145 (2018) 165–190.
- [30] B.A. Akhoon, S. Choudhary, H. Tiwari, A. Kumar, M.R. Barik, L. Rathor, R. Pandey, A. Nargotra, Discovery of a new donepezil-like acetylcholinesterase inhibitor for targeting Alzheimer's disease: computational studies with biological validation, J. Chem. Inf. Model. 60 (10) (2020) 4717–4729.
- [31] G. Kryger, I. Silman, J.L. Sussman, Structure of acetylcholinesterase complexed with E2020 (Aricept): implications for the design of new anti-Alzheimer drugs, Structure 7 (3) (1999) 297–307.
- [32] L. Peauger, R. Azzouz, V. Gembus, M.L. Tintas, J. Sopkova-de Oliveira Santos, P. Bohn, C. Papamicael, V. Levacher, Donepezil-based central acetyl-

- cholinesterase inhibitors by means of a "bio-oxidizable" prodrug strategy: design, synthesis, and *in vitro* biological evaluation, J. Med. Chem. 60 (13) (2017) 5909–5926.
- [33] H. Sugimoto, H. Ogura, Y. Arai, Y. Limura, Y. Yamanishi, Research and development of donepezil hydrochloride, a new type of acetylcholinesterase inhibitor, Jpn. J. Pharmacol. 89 (1) (2002) 7–20.
- [34] Z.M. Wang, P. Cai, Q.H. Liu, D.Q. Xu, X.L. Yang, J.J. Wu, L.Y. Kong, X.B. Wang, Rational modification of donepezil as multifunctional acetylcholinesterase inhibitors for the treatment of Alzheimer's disease, Eur. J. Med. Chem. 123 (2016) 282–297
- [35] F.S. Katz, S. Pecic, L. Schneider, Z. Zhu, A. Hastings, M. Luzac, J. Macdonald, D.W. Landry, M.N. Stojanovic, New therapeutic approaches and novel alternatives for organophosphate toxicity, Toxicol. Lett. 291 (2018) 1–10.
- [36] G.L. Ellman, K.D. Courtney, V. Andres, R.M. Feather-Stone, A new and rapid colorimetric determination of acetylcholinesterase activity, Biochem. Pharmacol. 7 (1961) 88–95.
- [37] M. Gupta, H.J. Lee, C.J. Barden, D.F. Weaver, The blood-brain barrier (BBB) score, J. Med. Chem. 62 (21) (2019) 9824–9836.
- [38] C.A. Lipinski, F. Lombardo, B.W. Dominy, P.J. Feeney, Experimental and computational approaches to estimate solubility and permeability in drug discovery and development settings, Adv. Drug. Deliv. Rev. 23 (1) (1997) 3–25.
- [39] D.F. Veber, S.R. Johnson, H.Y. Cheng, B.R. Smith, K.W. Ward, K.D. Kopple, Molecular properties that influence the oral bioavailability of drug candidates, J. Med. Chem. 45 (12) (2002) 2615–2623.
- [40] S. Pecic, M.A. McAnuff, W.W. Harding, Nantenine as an acetylcholinesterase inhibitor: SAR, enzyme kinetics and molecular modeling investigations, J. Enzyme Inhib. Med. Chem. 26 (1) (2011) 46–55.
- [41] M. Dixon, The determination of enzyme inhibitor constants, Biochem. J. 55 (1) (1953) 170–171.